Prediction of modes with dominant base roll and propeller twist in *B*-DNA poly(dA)-poly(dT)

L. Young, V. V. Prabhu, and E. W. Prohofsky
Department of Physics, Purdue University, West Lafayette, Indiana 47907

G. S. Edwards
Department of Physics and Astronomy, Vanderbilt University, Nashville, Tennessee 37235
(Received 3 April 1989; revised manuscript received 12 December 1989)

In solving the secular equation of a one-dimensional infinite lattice model of poly(dA)-poly(dT), we obtain dispersion relations. [The notation poly(dA)-poly(dT) means that one strand contains only adenine (A) bases, and the other only thymine (T) bases.] We solve the equation for consecutive refinements of the nonbonded force constants based on Raman, Brillouin, and neutron scattering and Fourier-transform infrared experiments in both polynucleotides and random sequence DNA. When these eigenvectors are examined for base roll and propeller twist, such characteristics are found to be dominant in modes around 50 cm^{-1}.

I. INTRODUCTION

The polymer poly(dA)-poly(dT) is a one-dimensional infinite lattice with the nucleotide pair adenine (A)–thymine (T) for a unit cell. Both bases are planar ringed structures. The orientation of these planar structures is described in terms of two parameters.[1] One is the angle between the bases in a pair, referred to as the propeller twist. The other is the base roll which describes the rotation of the base pair as a whole. We calculate the absolute base roll which is the change of angle the base pair, rolling as one unit, makes with the mean base pair plane. Structural investigations by the Klug[2] and Rich[3] groups of single crystals of DNA dodecamers have identified a "propeller twist" conformation for regions containing a homopolymeric run of A-T base pairs. Austin has suggested that propeller twist and base pair roll are temperature dependent in solutions of poly(dA)-poly(dT).[4] Liu *et al.*[5] suggest that the onset of these departures from a more regular structure could be soft mode mediated. To explore this possibility we examine the eigenvectors of our dynamical matrix for dominant base roll and propeller twist.

Forty-one atoms comprise the unit cell, the masses and charges of the hydrogen atoms being included in the heavy atoms to which they are attached. The resulting 123 modes range in frequency from 0.0 to 1700 cm^{-1}. The eigenvectors are from five different calculations, based on consecutive refinements of the nonbonded force constants[6–8] and also on two different coordinate refinements.[9,10] On average, for these calculations at zone center, 12.4% of the modes lie in the 0–100-cm^{-1} range, 6.7% in the 100–200-cm^{-1} range, 5.5% in the 200–300-cm^{-1} range, 8.3% in the 300–400-cm^{-1} range, and 67.1% above 400 cm^{-1}. The first refinement of the nonbonded force constants by Devi-Prasad and Prohofsky[6] is in agreement with the acoustic velocity of the compressional mode obtained by Brillouin scattering on randomly sequenced DNA.[11] The second nonbonded force-constant refinement, in addition, uses parameters from a calculation of the vibrational modes of the copolymer *B*-poly(dA-dC)-poly(dG-dT) (Ref. 7) which is fitted to neutron scattering on randomly sequenced DNA.[12] The final and most recent refinement[8] fits the van der Waals term to data from a Fourier-transform infrared experiment on a sample of poly(dA)-poly(dT) (Ref. 13). In all of our present homopolymer calculations,[8,13,14] we use this latest refinement, as it gives the most extensive agreement with experimental results. However, since we have available dispersion data from previous refinements and for the two different coordinate refinements, we should also like to record the effects of these changes on our results.

II. CALCULATION

The eigenvectors for these calculations are found as follows. The equation of motion[15] of the polymer is given by

$$(\underline{B}^{\dagger}\underline{F}\,\underline{B})q=\omega^2\mathbf{q}\ . \tag{1}$$

$\mathbf{q}$ are the eigenvectors, ω the eigenfrequencies, $\underline{F}$ the matrix of force constants of the internal coordinates of the lattice, and $\underline{B}$ the transformation matrix from internal coordinates to Cartesian coordinates. The force-constant matrix $\underline{F}$ can be considered as

$$\underline{F}=\underline{F}_V+\underline{F}_{\mathrm{NB}}\ . \tag{2}$$

$\underline{F}_V$ is the matrix of valence force constants refined from spectral data above 400 cm^{-1}.[16] In seeking to compare dispersion relations, that is, relationships between frequency and wavelength of the normal modes in the lattice, to experiment, we find that to the valence force constants $\underline{F}_V$ must be added nonbonded interactions $\underline{F}_{\mathrm{NB}}$ between a unit cell and its neighbors. The nonbonded in-

teraction consists of a Coulombic term and a van der Waals term, the specific form of which affects modes below 200 cm^{-1}.

A. Nonbonded interaction

Our present refinement of the nonbonded or long-range force constants is based on Brillouin and Fourier-transform infrared experiments as well as a copolymer model refined to fit neutron scattering data on random sequence DNA. We shall describe the three successive refinements of the nonbonded or long-range forces specified below as LRF1, LRF2, and LFR3. The specific form of both the Coulombic and van der Waals force needed for such correlation is also affected by the model assumed for both charges on the atoms and their position coordinates. Thus, in Table I, CR1 and CR2 refer to two different coordinate refinements from Arnott *et al.*[9,10] We use charges from Miller[17] in the first, second, fourth, and fifth columns of Table I and charges from Renugopalkrishnan *et al.*[18] in the third column. The Miller charges are reduced by 2.31 by comparison to experimentally determined charges.[19] In Eqs. (3), (4), and (5), e_i refers to the charge on atom i, r_{ij} to the distance between atoms i and j, and ϵ the dielectric constant. Two dielectric constants are required as some atoms affect each other through water and some through bases. Our earlier nonbonded or long-range force model LFF1 has

$$F_{ij}=\frac{\alpha|e_ie_j|}{(\epsilon_i\epsilon_j)^{1/2}r_{ij}^3}\ , \tag{3}$$

with a fitting parameter $\alpha=1.8$, the dielectric constant of water taken as 81.0, and the dielectric between bases being 6.0.[6] This reproduces the acoustic velocity of the compressional mode obtained by Brillouin scattering.[11] The third column of Table I is labeled LRF1a, since, as mentioned previously, different charges are used.

The nonbonded model LRF2 has

$$F_{ij}=\frac{2\eta|e_ie_j|}{(\epsilon_i\epsilon_j)^{1/2}r_{ij}^3}+\left[-\frac{42.0A}{r_{ij}^8}+BC^2e^{-Cr_{ij}}\right]\ . \tag{4}$$

Since Lee *et al.*[20] have indicated that the water dipole orientation time near the DNA polymer varies with frequency, we have improved our model of nonbonded interaction, by using a value of 9.0 for the dielectric constant of water. For the dielectric between the bases, we continue to use 6.0. $\eta=0.43$ which accounts for the scaling of the charges and a conversion factor to give the force constants in units of mdyn/A, for charges given in units of electronic charge and coordinates given in angstroms. The constants for the van der Waals term come from Eyster and Prohofsky,[15]

$$A=1.85\ ;$$

$$B=209.2\ ;$$

$$C=3.7\ .$$

This model is used by Prabhu *et al.*[7] for the DNA copolymer poly(dA-dC)-poly(dG-dT) in fitting the acoustic compressional mode to that observed in inelastic neutron scattering.[12]

Our third model LRF3 has

$$F_{ij}=\frac{2\eta|e_ie_j|}{(\epsilon_i\epsilon_j)^{1/2}r_{ij}^3}+\left[\frac{42A}{r_{ij}^8}\right]\ . \tag{5}$$

TABLE I. Frequency ranges (cm^{-1}) for base roll and propeller twist.

	CR1[a]-LRF3[b]		CR1-LRF3a[c]		CR1-LRF1a[d]		CR2[e]-LRF2[f]		CR2-LRF1[g]	
Calc.	Freq.	t_i^2	Freq.	t_i^2	Freq.	t_i^2	Freq.	t_i^2	Freq.	t_i^2
Twist										
	51.9	0.76	49.4	0.74	43.3	0.45				
Twist-adenine										
							43.4	0.51	43.5	0.55
			47.6	0.69					46.3	0.46
	49.9	0.70	49.4	0.75						
	51.9	0.76			52.0	0.73	53.4	0.61	65.1	0.61
Twist-thymine										
					43.3	0.88	43.4	0.77	43.5	0.46
			47.6	0.89					46.3	0.48
	49.9	0.86	49.4	0.84						
	51.9	0.81			52.0	0.46				
Roll										
	49.9	0.79	47.6	0.79	43.3	0.58	43.4	0.69		

[a]CR1 refers to the coordinate refinement of Ref. 9.
[b]LRF3 refers to Eq. (5) with $A=0.12$.
[c]LRF3a refers to Eq. (5) with $A=-0.048$.
[d]LRF1 refers to Eq. (1) with charges from Ref. 19. (Except for this column, all charges are from Ref. 18.)
[e]CR2 refers to the coordinate refinement of Ref. 10.
[f]LFR2 refers to Eq. (4).
[g]LRF1 refers to Eq. (1).

Here a distance-dependent dielectric[21] is used with the dielectric constant between atoms taken as 1.0 for a separation of 2 Å. The water dielectric rises to 9.0 at a distance of 10 Å, and the base dielectric rises to 6.0. $\eta=0.43$ as in LRF2. However, the van der Waals term has been simplified for fitting to data in the far-infrared region (50–115 cm^{-1}) measured by Fourier-transform infrared methods (Fig. 5 of Powell *et al.*).[22] Thus $A=0.12$. This latest model is the best fit to experimental data for poly(dA)-poly(dT). Initially, we had used a value $A=-0.048$ which we label LRF3a in the second column of Table I.

Because of the variation of water dipole orientation time with frequency, the dielectric constant is frequency dependent as well. For this reason, a value of 81.0 is used for the dielectric constant of water in reproducing the Brillouin scattering results (5–20-GHz range), and a value of 9.0 is used in reproducing inelastic neutron scattering data (THz region). Using the appropriate nonbonded force-constant matrix, $\underline{F}_{\rm NB}$, we diagonalize $\underline{B}^{\dagger}\underline{F}\,\underline{B}$ in Eq. (1) and obtain normalized eigenvectors and eigenvalues of the lattice. Depending on the nonbonded interaction used, the lowest-lying optical mode varies between 6 and 9 cm^{-1}. The next highest optical mode varies between 11 and 18 cm^{-1}. The lowest observed optical mode in Raman scattering is at 12 cm^{-1}.[23]

B. Absolute base roll and propeller twist

The components of an eigenvector interpret as the relative amplitudes of motion of all the atoms in the unit cell. These amplitudes are calculated in mass-weighted, Cartesian displacement coordinates. By convention the axis of roll or twist for the bases is through the pyrimidine C(6) atom and the purine C(8) atom. We construct a test vector with no displacement in the sugar phosphate (backbone) atoms but a roll or twist about the above-mentioned axis in the two bases. We mass weight this vector in the same way the eigenvectors are mass weighted, and then take the dot product of this test vector with all eigenvectors of the dynamical matrix (that is, an orthogonal and normalized set). If the dot product with the ith eigenvector is t_i',

$$\sum_i (t_i')^2=1 \ . \tag{6}$$

Those eigenvectors of the dynamical matrix, whose square of the inner product with the test vector is greater than 0.5, are interpreted as possessing in character the roll or twist of the test eigenvector.

III. RESULTS

We employed four kinds of test vectors.

1. A test vector with unit angular propeller twist between the two bases about the C(6)-C(8) axis. The results are displayed in the first row of Table I.

2. A test vector with unit angular displacement of adenine about the C(6)-C(8) axis with all other atoms at rest. The results are displayed in the second row of Table I.

3. A test vector with unit angular displacement of thymine about the C(6)-C(8) axis with all other atoms at rest. The results are displayed in the third row of Table I.

4. A test vector with unit base roll about the C(6)-C(8) axis with all atoms in the sugar phosphate backbone at rest. The results are displayed in the fourth row of Table I.

In each column of Table I, we specify first the modes which have the value of the square of inner product $t_i'^2$ greater than 0.5 and then the value of $t_i'^2$ itself. However, we must note one point. In order to detect the tendency of the bases to twist or roll, even when the backbone atoms have a large-amplitude motion, we keep only the part of the eigenvector representing the amplitude of the base atoms and normalize this new set. In this process, we lose the orthogonality of our set of eigenvectors and thus the relation in Eq. (6). For this reason, we denote the inner product of test vector with the new ith eigenvector as t_i instead of t_i'. (This change is not a problem for our study, since we are not interested in the actual amplitude of motion of the atoms so much as the tendency of the bases to twist.)

We notice that in all the models employed for the nonbonded forces, the dominant response of base roll or propeller twist is in the range 43–53 cm^{-1}. In each column

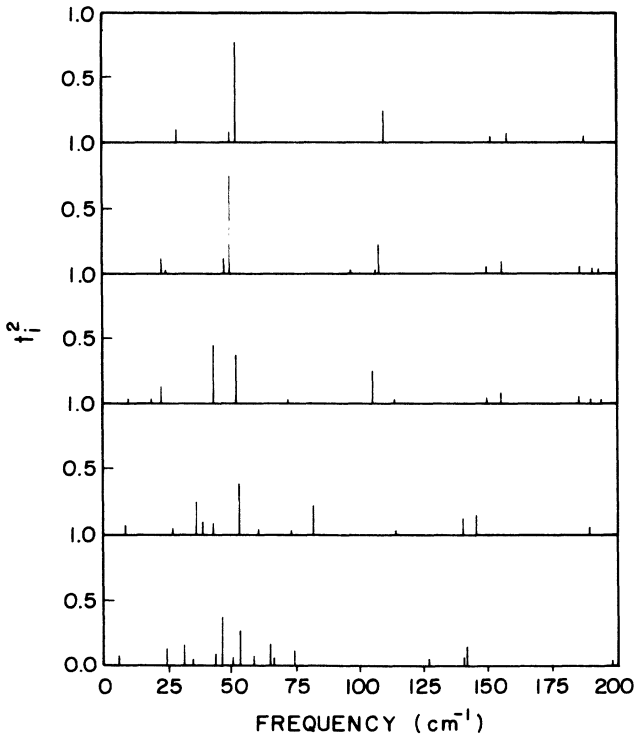

FIG. 1. Distribution of propeller twist modes in the 0–200-cm^{-1} range for each column of the first row in Table I. (Note: first row, the fourth and fifth columns of Table I are blank, since the square inner products for those calculations are less than 0.5 as seen here.)

of Table I, we see that either the adenine or the thymine base shows a tendency to rotate about the C(6)-C(8) axis. These details show the contribution of the separate motion of each base unit to the propeller twist and base roll. For example, in the first and second columns, we see that the thymine base contributes more to the propeller twist and base roll than the adenine base. That is, the propeller twist and base roll have larger projections onto the thymine-only twist.

In Fig. 1, we show the distribution of the propeller twist modes in the 0–200-cm^{-1} range. This figure corresponds to the first row of Table I; that is, starting from the top of Fig. 1, and counting downward, the first plot corresponds to propeller twist for CR1-LRF3. The second plot is for propeller twist, CR1-LRF3a; the third plot, for propeller twist, CR1-LRF1a; the fourth, for propeller twist, CR2-LRF2; and the fifth, for CR2-LRF1. The total number of modes in the 0–200-cm^{-1} region is 24 for the first three plots and 20 and 25 for the fourth and fifth plots, respectively. In those cases in which one mode has most of the propeller twist character, the other modes will have very small or zero t_i^2 and thus will not appear in the figure. Values for propeller twist are not given in the fourth and fifth columns of Table I, since the t_i^2 for these calculations is less than 0.5. However, we note that even for these calculations, the highest values of the t_i^2 are centered around 50 cm^{-1} (Fig. 1).

In comparing the first and second columns of Table I (also the upper two plots in Fig. 1), we see that the effect of adjusting A in Eq. (5) is a slight decrease in the frequencies of the modes in the 50-cm^{-1} range. In the other long-range force models (Fig. 1), the propeller twist character is less distinct for a particular mode. Instead, it appears to be shared over two or three modes.

In measuring the low-frequency Raman spectra of oriented fibers of poly(dA)-poly(dT), Liu *et al.*[5] report bands near 60 and 130 cm^{-1} which appear to "melt out" with prolonged laser exposure. One explanation[5] proposed is that the bands are associated with a temperature-dependent soft mode for the transition to a propeller twist conformation, and thus the bands disappear as the temperature of the sample rises with increased photon counts. The implication of the present calculation is that a mode in the 43–53-cm^{-1} range should be a candidate for this soft mode. This calculation also suggests a correlation between the experimentally observed mode near 135 cm^{-1} and the calculated modes in the 105–110-cm^{-1} range (Fig. 1).

ACKNOWLEDGMENTS

This project has been supported in part by U.S. Office of Naval Research Contract No. N00014-86-K-0252 and National Institutes of Health Grant No. GM24443.

[1]W. Saenger, *Principles of Nucleic Acid Structure* (Springer-Verlag, New York, 1984), p. 26.

[2]H. C. M. Nelson, J. T. Finch, B. F. Luisi, and A. Klug, Nature (London) **330**, 221 (1987).

[3]M. Coll, C. A. Frederick, A. H. J. Wang, and A. Rich, Proc. Natl. Acad. Sci. USA **84**, 8385 (1987).

[4]R. Austin (private communication).

[5]C. Liu, G. S. Edwards, S. Morgan, and E. Silberman, Phys. Rev. A **40**, 7394 (1989).

[6]K. V. Devi-Prasad and E. W. Prohofsky, Biopolymers **23**, 1795 (1984).

[7]V. V. Prabhu, W. K. Schroll, L. L. Van Zandt, and E. W. Prohofsky, Phys. Rev. Lett. **60**, 1587 (1988).

[8]L. Young, V. V. Prabhu, and E. W. Prohofsky, Phys. Rev. A **39**, 3173 (1989).

[9]S. Arnott, P. J. Campbell Smith, and R. Chandrasekaran, in *Handbook of Biochemistry and Molecular Biology,* 3rd ed., edited by G. D. Fasman (Chemical Rubber, Cleveland, 1975), Vol. 2, p. 411.

[10]R. Chandrasekaran and S. Arnott, in *Landolt-Börnstein Numerical Data and Functional Relationships in Science and Technology,* Vol. VII/1b of *Landolt-Börnstein,* edited by W. Saenger (Springer-Verlag, Berlin, 1989).

[11]S. M. Lindsay and J. Powell, in *Structure and Dynamics—Nucleic Acids and Proteins,* edited by E. Clementi and R. H. Sarma (Adenine, New York, 1983), p. 241.

[12]H. Grimm, H. Stiller, C. F. Majkrzak, A. Rupprecht, and U. Dahlborg, Phys. Rev. Lett. **59**, 1780 (1987).

[13]L. Young, V. V. Prabhu, and E. W. Prohofsky, Phys. Rev. A **40**, 5451 (1989).

[14]K. M. Awati and E. W. Prohofsky, Phys. Rev. A **40**, 497 (1989).

[15]J. M. Eyster and E. W. Prohofsky, Biopolymers **13**, 2505 (1974).

[16]K. C. Lu, E. W. Prohofsky, and L. L. Van Zandt, Biopolymers **16**, 2491 (1977).

[17]K. J. Miller, Biopolymers **18**, 959 (1979).

[18]V. Renugopalakrishnan, A. V. Lakshminarayanan, and V. Sashisekaran, Biopolymers **10**, 1159 (1971).

[19]D. A. Pearlman and S. H. Kim, Biopolymers **24**, 327 (1985).

[20]S. A. Lee *et al.*, Biopolymers **26**, 1637 (1987).

[21]A. J. Hopfinger, *Conformational Properties of Macromolecules* (Academic, New York, 1973), Chap. 2.

[22]J. W. Powell *et al.*, Phys. Rev. A **35**, 3929 (1987).

[23]Y. Tominaga *et al.*, J. Chem. Phys. **83**, 5972 (1985).